AAC Accepts, published online ahead of print on 8 December 2014
Antimicrob. Agents Chemother. doi:10.1128/AAC.03543-14
Copyright © 2014, American Society for Microbiology. All Rights Reserved.

AAC Accepts published online ahead of print

Novel Dengue virus NS2B/NS3 protease inhibitors

Hongmei Wu[1#], Stefanie Bock[2#], Mariya Snitko[2], Thilo Berger[1], Thomas Weidner[1], Steven Holloway[1], Manuel Kanitz[3], Wibke E. Diederich[3], Holger Steuber[4†], Christof Walter[5], Daniela Hofmann[2], Benedikt Weißbrich[2], Ralf Spannaus[2], Eliana G. Acosta[6], Ralf Bartenschlager[6,7], Bernd Engels[5], Tanja Schirmeister[1] and Jochen Bodem[2*]

[1]Institut für Pharmazie und Biochemie, Johannes Gutenberg-Universität Mainz, Germany
[2]Institut für Virologie und Immunbiologie, Julius-Maximilians-Universität Würzburg, Germany
[3]Institut für Pharmazeutische Chemie, Philipps-Universität Marburg, Germany
[4]LOEWE-Zentrum für Synthetische Mikrobiologie, Philipps-Universität Marburg, Germany
[5]Institut für Physikalische und Theoretische Chemie, Julius-Maximilians-Universität Würzburg, Germany
[6]Department of Infectious Diseases, Molecular Virology, Heidelberg University
[7]German Center for Infection Research, Heidelberg University
†Present address: Bayer Pharma AG, Lead Discovery Berlin – Structural Biology, Germany
[#]H. W. and S. B. contributed equally to the paper

*Corresponding author:
Jochen Bodem
Mailing address: Universität Würzburg, Institut für Virologie und Immunbiologie,
Versbacher Str. 7,
97078 Würzburg, Germany
Tel: +49-931-201-49558
Fax: +49-931-201-49553
e-mail: Jochen.Bodem@vim.uni-wuerzburg.de

AAC Accepts published online ahead of print

25 **ABSTRACT**

26 Dengue fever is a severe, widespread and neglected disease with more than 2 million diagnosed
27 infections per year. The Dengue virus NS2B/NS3 protease (PR) represents a prime target for rational
28 drug design. At the moment there are no clinical PR inhibitors (PIs) available. We have identified
29 diaryl (thio)ethers as candidates for a novel class of PIs. Here, we report the selective and non-
30 competitive inhibition of the serotypes 2 and 3 Dengue PR *in vitro* and in cells by benzothiazole
31 derivatives exhibiting IC_{50} values in the low micromolar range. Inhibition of DENV serotypes 1-3
32 replication was specific, since all substances neither influenced HCV, nor HIV-1 replication.
33 Molecular docking suggests binding at a specific allosteric binding site. In addition to the *in vitro*
34 assays a cell-based PR assay was developed to test these substances in a replication-independent way.
35 The new compounds inhibited the DENV PR with IC_{50} in the low micromolar or sub-micromolar
36 range in cells. Furthermore, these novel PIs inhibit viral replication at sub-micromolar concentrations.

37

38 **KEYWORDS.** Dengue virus, protease, rational antiviral drug design, protease inhibitor, diaryl
39 (thio)ether

AAC Accepts published online ahead of print

40 **INTRODUCTION**

41 Dengue viruses (DENV) are enveloped positive strand RNA viruses and belong to the family
42 Flaviviridae. DENV is the most important arthropod-borne viral infection. Over one third of the world
43 population lives in DENV endemic areas and an estimated 390 million infections occur every year. In
44 addition, the number of countries having experienced DENV epidemics has risen from 9 in 1970 to
45 more than 100 nowadays (1, 2). Furthermore, diagnosed infections across America, South-east Asia
46 and Western Pacific nearly doubled from 1.2 million in 2008 to over 2.3 million in 2010 (2). Four
47 different DENV serotypes were identified so far. Recently, evidence for an additional subtype has
48 been presented (3). Serotypes 1-4 are now prevalent in Asia, Africa and America and the endemic
49 regions are still increasing (4-6) endangering even Europe and the USA due to vector spread. DENV
50 infections can be associated with Dengue fever, but up to 88% of the infections remain inapparent (7).
51 These non-persistent infected patients serve beside persistently infected mosquitoes as virus reservoir.
52 Severe DENV infections and especially reinfections may lead to the dengue hemorrhagic fever and the
53 dengue shock syndrome with lethality up to 5% (2, 8, 9). There is neither a vaccination nor a specific
54 treatment for DENV infections.

55 The DENV genome contains a single open reading frame, which encodes the structural proteins
56 capsid, membrane precursor (prM), envelope and the non-structural (NS) proteins NS1, NS2, NS3,
57 NS4 and NS5 (10). Cellular proteases and the viral serine protease (PR) are responsible for cleaving
58 the viral precursor polyprotein into functional proteins. The DENV PR consists of the amino terminal
59 domain of the NS3 protein and requires NS2B, a 14kDa protein, as cofactor to form a stable complex.
60 This heterodimeric PR cleaves at the capsid-prM, NS2A/NS2B, NS2B/NS3, NS3/NS4A, NS4B/NS5,
61 internal NS2A, NS3 and NS4A cleavage sites (10, 11). PR inhibitors (PIs) were shown to be valuable
62 antiviral drugs especially in the treatment of HIV-1 and hepatitis C virus (HCV) (12-17). In case of
63 DENV, some already published substances showed inhibition of 50% in DENV replication in a mini
64 replicon system at submicromolar range (18) or inhibition to 10% of DENV replication with wild-type
65 virus at micromolar concentrations (19). Despite these promising developments, antiviral DENV
66 drugs are still not available.

AAC Accepts published online ahead of print

67 In this report, we describe the specific and selective inhibition of the DENV PR by diaryl
68 (thio)ethers. Evidence is provided for inhibition of the DENV-2 and -3 PR in vitro and for DENV-2
69 PR in cell culture. Furthermore, we show suppression of DENV-2 replication at submicromolar PI
70 concentrations.

71 **MATERIAL and METHODS**

72 **DENV-2/DENV-3 PR expression and purification.** Competent BL21Star *E. coli* (GE life
73 technologies) or BL21Gold(DE3) were transformed with either a DENV-2 PR encoding pET-28C (for
74 the DENV-2 enzyme used for fluorometric enzyme assays) (20), pET15b vector (for the DENV-2
75 enzyme used for microscale thermophoresis) (21) or a pGEX6P1 vector encoding the DENV-3 PR
76 (22). PR expression was induced by addition of 1 mM IPTG for 2 to 7 h at 37°C. Bacteria were lysed
77 by sonification in lysis buffer (50 mM NaH_2PO_4, 300 mM NaCl, 10 mM imidazole, pH 8.0; 100 µM
78 PMSF and 3.08 µM aprotinin). The DENV-2 PR was purified either using Ni-NTA-beads (Qiagen)
79 and native wash buffer (lysis buffer with 20 mM imidazole); elution buffer (lysis buffer with 250 mM
80 imidazole) or loaded on HisTrap FF [DENV-2] or on GSTrap FF [DENV-3](GE Healthcare) columns
81 and eluted using the particular lysis buffers (Supplementary Material) containing either 300 mM
82 imidazole [DENV-2] or 10 mM reduced glutathione [DENV-3]. The PR was further purified by size
83 exclusion chromatography. Protein amounts were determined by Bradford assay and verified by
84 Coomassie stained PAGE. DENV PR purity was analyzed by silver stained PAGE.

85 **Chemistry.** The synthesis of the compounds is described in the Supplementary information
86 (Supplementary Information and Supplementary Figures S1 and S2).

87 **Quantum mechanics computations**. Single point calculations as well as full geometry
88 optimizations with several different structures and corresponding frequency calculations were
89 performed on the B3LYP-D3/cc-pVDZ (23-28) level of theory as implemented in Turbomole
90 (Turbomole GmbH, Germany). Additional constrained geometry optimizations of the docking
91 structures were performed with the B3LYP functional and the cc-pVDZ basis sets using the Gaussian
92 09 program package (Gaussian Inc, USA). To obtain the relative energies of all conformers we

AAC Accepts published online ahead of print

93 performed single point B3LYP-D3/cc-pVDZ calculation on the geometries obtained from the
94 constrained optimizations.

95 **Molecular Docking.** For molecular docking of compounds **1–8**, the recently solved crystal structure
96 of DENV-3 PR in complex with the aldehyde inhibitor Bz-nKKR-H (pdb accession code 3U1I) was
97 used (22). Possible docking modes between ligands and the PR were studied using the FlexX docking
98 approach of the LeadIT 2.2.6 suite (BioSolveIt, Germany). Energies of compound structures were
99 minimized using the MOE software (Molecular Operating Environment, 2012.10). All water and
100 ligand molecules were deleted from the PR structure. The binding site was defined on a proper protein
101 pocket, which was shown to be a specific allosteric binding site for other non-competitive inhibitors
102 near the catalytic site (29).

103 **Fluorometric DENV PR assays.** For a preliminary screening of the substance library DENV-2 PR
104 assays using 100 µM of the fluorogenic substrate Boc-Gly-Arg-Arg-7-amino-4-methylcoumarin (20,
105 30) were performed. Assay conditions were taken from ref. (20). For the first screening approach
106 substrate hydrolysis was measured in absence (100 % enzyme activity) or presence of 50 µM
107 inhibitor. IC_{50}-values for selected compounds were determined measuring the increase of fluorescence
108 at 10 different PI concentrations ranging from 0 - 500 µM, 0 - 100 µM or 0 - 10 µM depending on
109 their inhibitory effects. Fluorescence increase resulting from the product AMC by substrate hydrolysis
110 was measured for 10 min after starting the reaction using an Infinite 200 PRO (Tecan, Männedorf,
111 Switzerland) (DENV-2) or a Saphire² plate reader (Tecan) (DENV-3) at room temperature with 380
112 nm excitation and 460 nm emission wavelengths. For DENV-3 PR assays 50 mM Tris-HCl, 1 mM
113 Chaps at pH 9.0 and 40 µM substrate (PhAc-Lys-Arg-Arg-AMC) were used. The final assay volume
114 was 200 µl. The reactions were started by adding either DENV-2 or DENV-3 PR to a final
115 concentration of 50 nM. Each assay was performed as triplicates at room temperature and IC_{50}-values
116 were calculated using GraFit (Erithacus Software Limited). IC_{50}-values were obtained by fitting the
117 residual enzyme activities to the 4-parameter IC_{50} equation:

$$y = \frac{y_{max} - y_{min}}{1 + (\frac{[I]}{IC_{50}})^s} + y_{min}$$

AAC Accepts published online ahead of print

118 (with y [dF/min] as the substrate hydrolysis rate, y_{max} as the maximum value of the dose-response
119 curve that is observed at very low inhibitor concentrations, y_{min} as the minimum value that is obtained
120 at high inhibitor concentrations, and s denotes the Hill coefficient (31)).

121 **HPLC-based enzyme assay.** See Supplementary Material.

122 **Binding assay based on microscale thermophoresis.** For compound **6** binding of the inhibitor to
123 the enzyme was quantified in a substrate-free assay using microscale thermophoresis (MST)
124 technology (32). For MST purified DENV-2/3 PR was labeled with the Monolith NTTM Protein
125 Labeling Kit Blue according to the supplied labeling protocol and 10 µl of a 95 nM stock solution of
126 DENV-2/3 PR were mixed with 10 µl of a serial dilution of compound **6** starting at 625 µM for
127 DENV-2 and 250 µM for DENV-3. Samples were diluted with buffers (for DENV-2 a 200 mM Tris-
128 HCl buffer pH 9.5 containing 30% glycerol; for DENV-3 a 50 mM Tris-HCl buffer pH 9.0 containing
129 1 mM CHAPS used) supplemented with DMSO at a final concentration of 5% (v/v) to ensure equal
130 DMSO concentrations. After incubation for 10 min samples were measured at an MST power of 40%
131 and a LED power of 20% with a laser-on time of 30 s and a laser-off time 5 s on a NanoTemper
132 Monolith NT.115 instrument using standard capillaries.

133 **DENV-2 replication, qRTPCR and cell culture based PR assays.** The DENV was obtained from
134 J. Schneider-Schaulies (Virology, Würzburg). The PR encoding region was amplified and sequenced
135 in order to confirm the serotype. In order to obtain high titer DENV, the virus was amplified by co-
136 culture techniques as described before for HIV-1 (33). Vero cells were infected and incubated for 3
137 days. One fifth of the infected cells and one fifth of the cell culture supernatants were used to infect
138 Vero cell. This process was repeated for 10times and the resulting supernatant stored at -80 °C. To
139 analyze inhibition of viral replication, Vero cells were pre-incubated with the components at
140 decreasing concentrations below the cell toxicity. The cells were subsequently infected with DENV-2
141 (MOI 0.5). Cellular supernatants were collected after four days, centrifuged at 2000 rpm for 5 min to
142 remove detached cells and titrated on Vero cells. These cells were fixed with 4% paraformaldehyde
143 three days after infection. To visualize infected cells an immunofluorescence staining was performed
144 with monoclonal anti-DENV-2 E antibodies. Bound antibodies were visualized with a Cy3 conjugated

AAC Accepts published online ahead of print

145 donkey anti-mouse antibody (1:500) (Jackson ImmunoResearch, USA). Stained infected cells were
146 counted using a fluorescence microscope and viral titers were calculated. All experiments were
147 performed in three independent triplicates. The significances of differences in infectivity compared to
148 wild-type maturation efficiencies were determined by the paired two-sample t-test.

149 To analyze the serotype specificity of the PIs DENV replication was monitored using a commercial
150 DENV qRTPCR kit (Genesig, Primerdesign LTD, Southampton, UK). Cells were infected with either
151 DENV-1 or DENV-2 (one genome copy per cell). The compounds were added subsequently and the
152 cells were incubated for 4 d. Cell culture supernatants were collected and centrifuged in order to
153 remove detached cells. Viral RNA was isolated using the QIAamp viral RNA mini kit, reverse
154 transcribed and amplified according to the manufactures' instructions.

155 A reporter system was constructed to analyze inhibition of the DENV-2 PR in cell culture. First, the
156 PR encoding sequence fused to a N-terminal FLAG Tag was introduced into a eukaryotic expression
157 vector, giving rise to the pDENV2-PR plasmid. Secondly, the DsRed2 open reading frame was
158 amplified with a sense primer encoding the DENV-2 NS2A/2B cleavage site. The amplicon was
159 introduced into the *gfp* encoding plasmid peGFP-C1 (Clontech) 3' of the *gfp* gene. The resulting
160 peGFPCSDsRed reporter plasmid encodes a GFP-NS2A/2B-DsRed fusion protein. HEK 293T cells
161 were co-transfected with both the PR expression plasmid pDENV2-PR and the peGFPCSDsRed
162 reporter. PIs were added directly after transfection. Cells were harvested 2 d post-transfection and
163 lysed in RIPA buffer (150 mM NaCl, 1% NP40, 0.5% deoxycholate, 0.1% SDS, 50 mM Tris pH 8.0).
164 Three independent Western Blots of each of the triplicate samples were used to calculate relative
165 substrate and product amounts using AIDA software package (GE Healthcare). All experiments were
166 repeated at least three times. The significances of differences in processing compared to wild-type
167 maturation efficiencies were determined by the paired two-sample t-test. Expression of the viral PR
168 was monitored by anti-FLAG Tag Western blotting using monoclonal anti-FLAG M2 antibodies
169 (Sigma-Aldrich).

170 **HIV-1 replication assay.** Viruses were produced by transfection of HEK 293T cells with proviral
171 plasmid pNL4-3 encoding infectious HIV-1 subtype B as described before (34). Viral titers were

AAC Accepts published online ahead of print

172 determined on TZM-bl indicator cells (CD4+, CCR5+, CXCR4+ HeLa cells) in single cycle infections
173 by serial dilutions of the cell culture supernatants as previously described (33, 34). Briefly, cell culture
174 supernatants were collected, centrifuged (1500 rpm, 5 min) to remove infected HEK 293T cells, and
175 titrated in serial dilutions on TZM-bl cells (96-well plate, $2x10^4$ cells per well). TZM-bl cells carry a
176 stably integrated copy of a HIV LTR promoter driving a *lacZ* gene. Two days post-infection, TZM-bl
177 cells were fixed with ice-cold methanol/acetone for 5 min followed by a β-Galactosidase stain, using
178 X-gal as substrate. Stained cells were counted and the viral titers were calculated.

179 **HCV replication assay.** Huh7.5 cells stably expressing the Firefly luciferase reporter gene
180 (Huh7.5-Fluc) were transfected by electroporation with *in vitro* transcribed RNA of the fully
181 functional *Renilla* luciferase-encoding reporter virus genome JcR2a (35). DMSO or different
182 concentrations of the compounds were added to the cells immediately after transfection. After 72 h of
183 incubation virus replication and cell viability were determined by measuring *Renilla* luciferase (Rluc)
184 and Firefly luciferase (Fluc) activity from cell lysates, respectively. Production of infectious particles
185 from transfected cells was determined by infection of naïve Huh7.5 cells with supernatants collected
186 from transfected cells and quantification of Rluc activity 72 h later. Experiments were performed three
187 times in triplicate (or sextuplicate in the case of DMSO treated cells). The HCV protease inhibitor
188 Boceprevir served as a positive control (36).

189 **Cell toxicity test.** To exclude toxic side effects of the PIs the cell survival and metabolism was
190 measured by a cell proliferation assay (Promega, Germany). Vero and HEK 293T cells ($2x10^4$) were
191 incubated with decreasing amounts of compounds solubilized in DMSO or with DMSO alone as
192 control. The assays were performed in triplicates according to the manufacturer's instructions. After
193 four days 20 µl of the MTS substrate were added, cells were further incubated for 90 min and the
194 OD_{490} was measured. Substance concentrations inhibiting the MTS substrate conversation were
195 excluded from further analyses.

196 **RESULTS AND DISCUSSION**

AAC Accepts published online ahead of print

197 **Inhibitor Design, Docking, and PR Inhibition.** To identify new chemical scaffolds for inhibitors
198 of the DENV PR an in house library consisting of approximately 250 compounds was screened at 50
199 μM. A previously described DENV-2 PR assay was used to analyze the substance library using a
200 fluorogenic Boc-GRR-AMC substrate (20, 30). By this assay an active key substance (compound **1**)
201 was discovered to inhibit the DENV-2 PR about 35% at 50 μM (Table 1). In a first approach to
202 improve affinity the thiophene moiety was replaced by alkyl chains or other (hetero)aromatic ring
203 systems, and the amide moiety was replaced by an ester or amine function. The diaryl thioethers were
204 prepared in a two-step synthesis (Table S1). HBTU served as coupling reagent for condensation of the
205 respective phenyl thiobenzoic acid with the amine parts of the inhibitors. Phenyl thiobenzoic acids
206 were prepared by nucleophilic aromatic substitution reaction from corresponding arylmercaptans and
207 arylhalides (37, 38).

208 Thus, we obtained a small series of new compounds (Supporting Information). Replacement of the
209 amide linker by an amine or ester group led to loss of activity, and also compounds with alkyl chains
210 instead of the thiophene moiety turned out to be inactive. Among the new compounds with other
211 heteroaromatic moieties PI **2** with nitro-substituted benzothiazol fragment was identified as the most
212 potent (Table 1, Supporting Information and Supporting Information Figure S1). In a next step the
213 position of the thioether fragment was changed from ortho- to para- or meta-position. Furthermore, the
214 thioether moiety was replaced by a methylene group, and the nitro group at the phenyl ring was
215 replaced by hydrogen, primary amine, or a trifluoromethyl group. Among these new compounds the
216 meta-substituted dinitro derivative **4** and the trifluoromethyl derivative **3** exhibited an improved
217 inhibition (Supporting Information Figure S1). In order to explain these structure-activity relationships
218 and to propel optimization forward on a rational basis we determined the inhibition mechanisms of the
219 original lead compound **1**, and the, to that point, most active inhibitor **3**. Both compounds were found
220 to be non-competitive with respect to the substrate. This was shown by determination of IC_{50} values at
221 different substrate concentrations (20, 50, 100, 200 mM), and, the other way round, by determination
222 of K_m and V_{max} values at various inhibitor concentrations. The first assays provided no significant
223 differences of IC_{50} values, and plots from the second assays showed typical non-competitive graphs
224 with decreasing V_{max} values and nearly constant K_m values at increasing concentrations [I] of inhibitor

AAC Accepts published online ahead of print

225 **3** ([I] = 0 μM: V_{max} ΔF/min // K_m μM = 52 // 75; [I] = 5 μM: 56 // 112; [I] = 25 μM: 32 // 108; [I] = 50
226 μM: 21 // 128; [I] = 75 μM: 14 // 95). Additionally, to exclude false positive results due to quenching
227 of the fluorescence of the hydrolysis product AMC by the nitro aromatics we determined inhibition of
228 the DENV-2 PR by compounds **2** and **3** using a semi-quantitative HPLC assay (Supporting
229 Information), which confirmed the inhibition of substrate hydrolysis observed with compound **2** and **3**
230 (~70 - 75% inhibition in the HPLC assay vs. ~70% inhibition in fluorescence assay).

231 The non-competitive inhibition raised the question of the binding region within the enzyme.
232 Previously a specific allosteric binding site for non-competitive and non-peptidic inhibitors has been
233 proposed. This deep binding pocket is located behind the active site (Ser135, Asp175, His51) and
234 mainly formed by the amino acids Trp89, Thr120, Gly121, Glu122, Ile123, Gly124, Gly164, Ile165,
235 Ala166, Gln167 on the one side and Lys73, Lys74, Asn152, Val78, Gly82, Met84 on the other side,
236 the last three of which are NS2B derived (Figure 1).

237 This binding pocket was taken for docking studies with compound **3** using the FlexX docking
238 approach of the LeadIT 2.2.6 suite with the recently solved crystal structure of DENV-3 PR in
239 complex with the aldehyde inhibitor Bz-nKKR-H (pdb accession code 3U1I) (22). The structure of the
240 DENV-3 PR was taken since both PRs show a high degree of similarity and the used DENV-3 PR
241 structure is the only available structure of a DENV PR in complex with a low-molecular weight
242 inhibitor.

243 Since diaryl thioethers are flexible compounds in respect to their thioether bond, quantum chemical
244 computations were performed in order to confirm that conformations obtained by docking studies are
245 plausible and this is indeed the case (Supporting Information). For compound **3** pose 3 is predicted to
246 be only about 1-5 kcal/mol higher than the global minima of the molecule, which is stabilized by
247 intramolecular π-π interactions. This energy difference can easily be compensated by inhibitor-enzyme
248 interactions. Pose 1 and 2 seem to be higher in energy since the amide unit is not or only partially in
249 conjugation with the other aromatic rings (see Supporting Information and Supporting Information
250 Figure S3).

AAC Accepts published online ahead of print

251 The docking studies proposed an interaction of the nitro group of compound **3** to the side chain of
252 Asn152 (Figure 2). In order to verify this binding mode by addressing additional possible binding
253 partners within the allosteric pocket we introduced a hydroxyl group adjacent to nitro group. This
254 should enable an additional hydrogen bond with the oxygen of the backbone carbonyl group in
255 Asn152. Additionally, instead of the nitro group a carboxylic acid function (compound **5**) or a second
256 hydroxyl group (compound **8**) were introduced to reduce possible quenching effects in the PR assays,
257 but to maintain the possible interaction to Asn152. While introduction of an acid and a hydroxyl
258 function at the benzothiazole moiety did not lead to improved affinity (compound **5**), the dihydroxy
259 substituted inhibitor **8** was found to be highly active with an IC_{50} value of 3.6 µM. Also this PI was
260 shown to be a non-competitive inhibitor. It has to be mentioned that despite the catechol structure the
261 compound is stable and not sensitive to oxidation. The docking studies with this inhibitor propose
262 interactions of one hydroxyl group with the side chain of Asn152 and with the backbone of Lys74, and
263 an interaction of the other hydroxyl group with Lys73 (Figure 2).

264 In agreement with the proposed binding mode the dimethoxy substituted compound **7** is not active
265 (10% inhibition at 50 µM). Also the derivatives with only one hydroxyl group are less active
266 corroborating the docking studies (see Supporting Information and Supporting Information Table S1).
267 Further docking studies proposed replacement of the trifluoromethyl substituted phenyl ring by a
268 hydroxyl substituted naphthyl moiety and replacement of the sulphur of the thioether bridge by oxygen
269 (Figure 3). This yielded compound **6**, which was shown to be a non-competitive inhibitor with an IC_{50}
270 value of ca. 4 µM. For that compound binding studies using microscale thermophoresis were
271 performed (Supporting Information Figure S4). Since these studies need labeling of the protein we
272 used the more stable mutant of the DENV-2 PR. With this substrate-independent binding assay we
273 found a dissociation constant of K_D = 15.2 µM, which confirms the fluorometric enzyme assays
274 (Supporting Information Figure S4).

275 For selected compounds, namely **1, 2, 3, 5, 6, 7** and **8**, the inhibition of the PR of the serotype 3
276 virus was tested. With the exception of compound **8** DENV-3 PR is more sensitive to the inhibitors
277 with derivative **6** which is the most active one against DENV-2 PR being also the most potent DENV-

AAC Accepts published online ahead of print

278 3 PI (IC_{50} = 1 µM). This also underlines the results of the docking studies, which were done with the
279 structure of DENV-3 PR.

280 **Toxicity and antiviral Activities.** Next, we analyzed inhibition of the viral replication by the PIs.
281 In order to exclude toxic side effects of the substances the cell survival and metabolism was measured
282 by a cell proliferation assay. Vero cells were incubated with decreasing amounts of the PIs solubilized
283 in DMSO or with DMSO alone as control (Table 1). Substance concentrations inhibiting the MTS
284 substrate conversation were excluded from further analyses. Substance **2** was not tested in cellular
285 assays, since it exhibited toxicity at concentrations below 1 µM (Table 1 and Supporting Information
286 Figure S5). Cell death due to cytotoxicity of the compounds was not observed at concentrations of
287 30µM. Higher concentration were not analyzed in cell culture.

288 To analyze inhibition of viral replication, Vero cells were pre-incubated with the PIs at decreasing
289 concentrations below the cell toxicity (Table 1 and Supporting Information Figure S5) and
290 subsequently infected with DENV-2. Cellular supernatants were collected after four days and titrated
291 on Vero cells. Virus infected cells were visualized by immunofluorescence staining and viral titers
292 were calculated (Table 1). All PIs did significantly decrease viral replication. Furthermore, substances
293 **3** and **4** inhibited viral replication more than 3 orders of magnitude at 1 µM and 3 µM, respectively
294 (Figure 4). This indicates that the PIs described here, except **2** and **8**, suppressed viral replication quite
295 efficiently at low micromolar or even submicromolar concentrations. Especially the low EC_{50} values
296 for compounds **3, 4, 5, 6** and **8** showed that we have identified inhibitors of DENV-2 replication.

297 In order to analyze, whether the compounds are able to inhibit PR of other DENV serotypes, effects
298 on replication was determined with DENV-1. Cells were infected with DENV-1 or DENV-2 in the
299 presence of the most effective compounds **3** and **4**. Viral replication was determined by quantification
300 of viral RNA genomes in the cellular supernatants by qRTPCR. Both, compounds **3** and **4** decreased
301 DENV-2 genome copies to 27% and 3.1% of the DMSO control, and DENV-1 genome copies to 10%
302 and 3.5% indicating that DENV-1 exhibits a similar sensitivity to both substances (Figure 4). These
303 results together with the results of the *in vitro* PR analyses provide evidence that compounds **3** and **4**
304 inhibit at least replication or PRs of DENV-1, DENV-2 and DENV-3.

AAC Accepts published online ahead of print

305 Interestingly the dimethoxy derivative **7** also exhibits antiviral activity against DENV-2 while it is
306 inactive against DENV-2 PR in the fluorometric enzyme assay (Table 1 and Figure 4). Vice versa, the
307 dihydroxy derivative **8** displays good inhibition of PR of serotypes 2 and 3, but is not active in cells at
308 concentrations below 3 μM. This observation leads to the hypotheses that compound **7** may act like a
309 prodrug being demethylated in cells yielding to the more potent dihydroxy derivative. This hypothesis
310 is supported by the fact that compound **7** inhibits DENV-1 replication as well (Figure 4) and the PR in
311 the cell-based assay (see below).

312 To further exclude that effects of our compounds on DENV-2 replication are due to cytotoxicity and
313 to prove the specificity of the observed inhibition of DENV-2 replication, we analyzed influences of
314 the PIs on HIV-1 replication. HIV-1 encodes an aspartate PR, which is neither in regard to its structure
315 nor to its substrate specificity similar to the DENV-PR. Thus, DENV PIs should not influence HIV-1
316 replication. HEK 293T cells were transfected with the proviral HIV-1 plasmid pNL4-3 and PIs were
317 added at concentrations above the EC_{50}. Viral supernatants were collected 2 days post transfection and
318 titrated on TZM-bl indicator cells (Figure 5). TZM-bl indicator cells encoded a LacZ gene controlled
319 by the HIV-1 LTR promoter. Infected cells were identified by β-galactosidase stain. None of the PIs
320 influenced HIV-1 replication excluding cellular toxicity and unspecific inhibition of the HIV-1 PR.

321 To analyze the specificity of compounds, we determined antiviral activity against HCV, another
322 member of the family *Flaviviridae*. Human hepatoma cells expressing a firefly luciferase reporter that
323 was used to measure cytotoxicity (not shown) (Huh7.5-FLuc), were transfected with a *Renilla*
324 luciferase (RLuc)-encoding HCV reporter genome (JcR2a; Fig. 6A). After 72 h, virus replication was
325 assessed by quantification of RLuc activity in transfected cells (Fig. 6B). To determine virus titers,
326 naïve Huh7.5 cells were inoculated with culture supernatants collected 72 h after transfection and
327 RLuc expression was determined 3 days later (Figure 6C). None of the compounds influenced HCV
328 replication or production of infectious particles, showing that the PIs are specific for DENV and
329 inactive against the related HCV.

330 **Inhibition of the DENV PR in cell culture.** To measure inhibition of the DENV-2 PR in cells
331 quantitatively and without any influences of the viral replication, such as additional replication cycles

AAC Accepts published online ahead of print

332 etc. a PR reporter system was constructed. The coding regions of *gfp* and *dsred2* were fused and a
333 NS2A/NS2B cleavage site was inserted by PCR (Figure 7). Cleavage of this GFP-NS2A/B cleavage
334 site-DsRed2 fusion protein by the DENV-2 PR would result in separated GFP and DsRed proteins.
335 HEK 293T cells were transfected with the reporter plasmid alone or in combination with a pDENV2-
336 PR expression plasmid. To monitor expression of the DENV PR a N-terminal M2 FLAG Tag was
337 added by PCR. Cleavage of the substrate was analyzed by quantitative Western blotting using anti-
338 GFP antibodies (Figure 7 and Supporting Information Figure S6). Determination of GAPH amounts
339 served as loading control. Expression of the substrate alone resulted in the expected protein of 55 kDa
340 protein. Co-expression of the DENV PR led to substrate cleavage of about 75%. Instead of the
341 expected single GFP derived product band, cleavage of the reporter fusion protein resulted in two
342 product bands (Figure 7). Therefore, we analyzed whether GFP was cleavage by the DENV-2 PR
343 (Supporting Information Figure S7) and could show that DENV-2 indeed cleaves the GFP protein at a
344 potential cleavage site KRDH. The lead substance **1** inhibited viral PR activity in cell culture already
345 with an IC_{50} at 15.6 µM. The optimized derivatives resulted in IC_{50} values in the low micromolar or
346 even submicromolar range (Table 1, Figure 7 and Supporting Information Figure S6). The high
347 inhibition of replication in comparison to the IC_{50} values for PR inhibition in cell culture could
348 indicate that an almost complete processing of viral proteins is required for viral infectivity. Similar
349 discrepancies between EC_{50} and IC_{50} values were observed by others, but attributed to the enzyme-
350 based DENV PR assay (18). Furthermore, our result might suggest that the PIs are enriched in cells.
351 Thus, concentrations less than the IC_{50} in cell culture led to the inhibition of viral replication.

352 Comparing the inhibition of the isolated proteases (column 1 and 2 in Table 1) with antiviral activity
353 (column 4) and PR inhibition in cell culture (column 5), no good correlation can be found between PR
354 inhibition (columns 1 and 2) and inhibition of viral replication (column 4) or PR in cell culture
355 (column 5). However, a very good correlation (Figure 8) can be found between antiviral activity
356 (column 4) and PR inhibition in cell culture (column 5) indicating that indeed the PR inhibition is the
357 main reason for the antiviral activity of the compounds, and furthermore substantiating the hypothesis
358 that the dimethoxy substituted compound **7** which is not active against the isolated proteases maybe a
359 prodrug for the dihydroxy compound **8**. On the other hand, these results show that for rational design

AAC Accepts published online ahead of print

360 of new PR inhibitors, both assays are necessary, the determination of inhibition of isolated proteases in
361 order to verify the docking hypotheses, and the determination of PR inhibition in cell culture which
362 can be used to predict the antiviral activity.

363 By analyzing influences of the PR inhibition in cell culture on DENV replication, a high sensitivity
364 of viral replication compared to the cell culture based cleavage assay was observed (Table 1 and
365 Figure 7). These results indicate that already partial inhibition of processing is detrimental for DENV,
366 which is similar to partial inhibition of HIV-1 maturation, which results in an almost complete
367 reduction of viral replication (39). Other viruses, such as foamy viruses, tolerate up to 40% of non-
368 processed proteins without any influences on viral replication (40). On the other hand, since the cell
369 culture based cleavage reporter system uses the NS2B/NS3 cleavage site, which was shown to be the
370 most efficient one, it can be assumed that the PIs will block less efficient cleavage sites at lower EC_{50}.

371 In summary, we describe a novel class of DENV-2/3 PR inhibitors with an inhibition of the PR *in*
372 *vitro* and *in vivo*, which are shown to inhibit viral replication. Our substances may serve as promising
373 lead-compounds for further studies and optimization.

374 **ACKNOWLEDGMENT**

375 We would like to thank A. Kucharski (University of Würzburg, Institute of Pharmacy and Food
376 Chemistry), S. Mährlein and U. Nowe (University of Mainz, Institute of Pharmacy and Biochemistry)
377 for technical and the University of Mainz for financial support. C.W. was supported by the
378 Studienstiftung des Deutschen Volkes, T. S. and B. E. by the DFG (SFB630). The DENV-2 PR
379 bacterial expression plasmid was kindly provided by C. Klein and C. Steuer (University of
380 Heidelberg) and the anti-DENV-2 E antibodies and Dengue viruses by J. Schneider-Schaulies
381 (University of Würzburg).

382 **ABBREVIATIONS**

383 AMC, 7-Amino-4-methylcoumarin; DENV, Dengue virus; DMSO, Dimethylsulfoxid; HBTU,
384 N,N,N′,N′-Tetramethyl-O-(1H-benzotriazol-1-yl)uronium hexafluorophosphate; HIV, human

AAC Accepts published online ahead of print

385 immunodeficiency virus; MOI, multiplicity of infection; MST, Microscale Thermophoresis; NS, non-
386 structural, PI, protease inhibitor; PR, protease
387

AAC Accepts published online ahead of print

388 **REFERENCES**

389 1. **Bhatt S, Gething PW, Brady OJ, Messina JP, Farlow AW, Moyes CL, Drake JM,**
390 **Brownstein JS, Hoen AG, Sankoh O, Myers MF, George DB, Jaenisch T, Wint GR,**
391 **Simmons CP, Scott TW, Farrar JJ, Hay SI.** 2013. The global distribution and burden of
392 dengue. Nature **496:**504-507.
393 2. **World-Health-Oraganization** November 2012 2012, posting date. Dengue and severe
394 dengue Fact sheet no 117. WHO media centre. [Online.]
395 3. **Normile D.** 2013. Tropical medicine. Surprising new dengue virus throws a spanner in disease
396 control efforts. Science **342:**415.
397 4. **Messer WB, Gubler DJ, Harris E, Sivananthan K, de Silva AM.** 2003. Emergence and
398 global spread of a dengue serotype 3, subtype III virus. Emerg Infect Dis **9:**800-809.
399 5. **Streit JA, Yang M, Cavanaugh JE, Polgreen PM.** 2011. Upward trend in dengue incidence
400 among hospitalized patients, United States. Emerg Infect Dis **17:**914-916.
401 6. **Guzman MG, Halstead SB, Artsob H, Buchy P, Farrar J, Gubler DJ, Hunsperger E,**
402 **Kroeger A, Margolis HS, Martinez E, Nathan MB, Pelegrino JL, Simmons C, Yoksan S,**
403 **Peeling RW.** 2010. Dengue: a continuing global threat. Nat Rev Microbiol **8:**S7-16.
404 7. **Endy TP, Anderson KB, Nisalak A, Yoon IK, Green S, Rothman AL, Thomas SJ,**
405 **Jarman RG, Libraty DH, Gibbons RV.** 2011. Determinants of inapparent and symptomatic
406 dengue infection in a prospective study of primary school children in Kamphaeng Phet,
407 Thailand. PLoS Negl Trop Dis **5:**e975.
408 8. **Luz PM, Vanni T, Medlock J, Paltiel AD, Galvani AP.** 2011. Dengue vector control
409 strategies in an urban setting: an economic modelling assessment. Lancet **377:**1673-1680.
410 9. **Guzman MG, Kouri G.** 2002. Dengue: an update. Lancet Infect Dis **2:**33-42.
411 10. **Lindenbach BD, Thiel H-j, Rice CM.** 2007. Flaviviridae: The viruses and their replication
412 p. 1101-1152. *In* Knipe DK, Howley DM (ed.), Fields Virology, vol. 1. Wolters Kluwer,
413 Philadelphia.
414 11. **Bera AK, Kuhn RJ, Smith JL.** 2007. Functional characterization of cis and trans activity of
415 the Flavivirus NS2B-NS3 protease. J Biol Chem **282:**12883-12892.
416 12. **Jacobson IM, McHutchison JG, Dusheiko G, Di Bisceglie AM, Reddy KR, Bzowej NH,**
417 **Marcellin P, Muir AJ, Ferenci P, Flisiak R, George J, Rizzetto M, Shouval D, Sola R,**
418 **Terg RA, Yoshida EM, Adda N, Bengtsson L, Sankoh AJ, Kieffer TL, George S,**
419 **Kauffman RS, Zeuzem S, Team AS.** 2011. Telaprevir for previously untreated chronic
420 hepatitis C virus infection. N Engl J Med **364:**2405-2416.
421 13. **Poordad F, McCone J, Jr., Bacon BR, Bruno S, Manns MP, Sulkowski MS, Jacobson**
422 **IM, Reddy KR, Goodman ZD, Boparai N, DiNubile MJ, Sniukiene V, Brass CA,**
423 **Albrecht JK, Bronowicki JP, Investigators S-.** 2011. Boceprevir for untreated chronic HCV
424 genotype 1 infection. N Engl J Med **364:**1195-1206.
425 14. **Matthews SJ, Lancaster JW.** 2012. Telaprevir: a hepatitis C NS3/4A protease inhibitor. Clin
426 Ther **34:**1857-1882.
427 15. **Pearlman BL.** 2012. Protease inhibitors for the treatment of chronic hepatitis C genotype-1
428 infection: the new standard of care. Lancet Infect Dis **12:**717-728.
429 16. **Kohl NE, Emini EA, Schleif WA, Davis LJ, Heimbach JC, Dixon RA, Scolnick EM, Sigal**
430 **IS.** 1988. Active human immunodeficiency virus protease is required for viral infectivity. Proc
431 Natl Acad Sci U S A **85:**4686-4690.
432 17. **Panel-on-Antiretroviral-Guidelines-for-Adults-and-Adolescents** 2012, posting date.
433 Guidelines for the use of antiretroviral agents in HIV-1-infected adults and adolescents.
434 Department of Health and Human Services. AIDSinfo Department of Health and Human
435 Services U.S. [Online.]
436 18. **Yang CC, Hsieh YC, Lee SJ, Wu SH, Liao CL, Tsao CH, Chao YS, Chern JH, Wu CP,**
437 **Yueh A.** 2011. Novel dengue virus-specific NS2B/NS3 protease inhibitor, BP2109,
438 discovered by a high-throughput screening assay. Antimicrob Agents Chemother **55:**229-238.
439 19. **Nitsche C, Schreier VN, Behnam MA, Kumar A, Bartenschlager R, Klein CD.** 2013.
440 Thiazolidinone-peptide hybrids as dengue virus protease inhibitors with antiviral activity in
441 cell culture. J Med Chem **56:**8389-8403.

AAC Accepts published online ahead of print

20. **Steuer C, Heinonen KH, Kattner L, Klein CD.** 2009. Optimization of assay conditions for dengue virus protease: effect of various polyols and nonionic detergents. J Biomol Screen **14:**1102-1108.
21. **D'Arcy A, Chaillet M, Schiering N, Villard F, Lim SP, Lefeuvre P, Erbel P.** 2006. Purification and crystallization of dengue and West Nile virus NS2B-NS3 complexes. Acta Crystallogr Sect F Struct Biol Cryst Commun. **62:**157-162.
22. **Noble CG, Seh CC, Chao AT, Shi PY.** 2012. Ligand-bound structures of the dengue virus protease reveal the active conformation. J Virol **86:**438-446.
23. **Grimme S, Antony J, Ehrlich S, Krieg H.** 2010. A consistent and accurate ab initio parametrization of density functional dispersion correction (DFT-D) for the 94 elements H-Pu. J Chem Phys. **132:**154104.
24. **Dunning JTH.** 1989. Gaussian Basis Sets for Use in Correlated Molecular Calculations. I. The Atoms Boron through Neon and Hydrogen. J. Chem. Phys **90:**1007-1023.
25. **Vosko SH, Wilk L, Nusair M.** 1980. Accurate spin-dependent electron liquid correlation energies for local spin density calculations: a critical analysis. Can. J. Phys. **58:**1200-1211.
26. **Becke AD.** 1988. Density-functional exchange-energy approximation with correct asymptotic behavior. Physical review. A **38:**3098-3100.
27. **Lee C, Yang W, Parr RG.** 1988. Development of the Colle-Salvetti correlation-energy formula into a functional of the electron density. Physical review. B, Condensed matter **37:**785-789.
28. **Becke AD.** 1993. Density-functional thermochemistry. III. The role of exact exchange. J. Chem. Phys. **98:**5648-5652.
29. **Othman R, Kiat TS, Khalid N, Yusof R, Newhouse EI, Newhouse JS, Alam M, Rahman NA.** 2008. Docking of noncompetitive inhibitors into dengue virus type 2 protease: understanding the interactions with allosteric binding sites. J Chem Inf Model **48:**1582-1591.
30. **Chanprapaph S, Saparpakorn P, Sangma C, Niyomrattanakit P, Hannongbua S, Angsuthanasombat C, Katzenmeier G.** 2005. Competitive inhibition of the dengue virus NS3 serine protease by synthetic peptides representing polyprotein cleavage sites. Biochem Biophys Res Commun **330:**1237-1246.
31. **Ludewig S, Kossner M, Schiller M, Baumann K, Schirmeister T.** 2010. Enzyme kinetics and hit validation in fluorimetric protease assays. Curr Top Med Chem **10:**368-382.
32. **Jerabek-Willemsen M, Wienken CJ, Braun D, Baaske P, Duhr S.** 2011. Molecular interaction studies using microscale thermophoresis. Assay Drug Dev Technol. **9:**342-353.
33. **Cígler P, Kozísek M, Rezácová P, Brynda J, Otwinowski Z, Pokorná J, Plesek J, Grüner B, Dolecková-Maresová L, Mása M, Sedlácek J, Bodem J, Kräusslich H, Král V, Konvalinka J.** 2005. From nonpeptide toward noncarbon protease inhibitors: metallacarboranes as specific and potent inhibitors of HIV protease. Proc Natl Acad Sci U S A **102:**15394-15399.
34. **Kozisek M, Henke S, Saskova KG, Jacobs GB, Schuch A, Buchholz B, Müller V, Kräusslich HG, Rezacova P, Konvalinka J, Bodem J.** 2012. Mutations in HIV-1 gag and pol compensate for the loss of viral fitness caused by a highly mutated protease. Antimicrob Agents Chemother **56:**4320-4330.
35. **Reiss S, Rebhan I, Backes P, Romero-Brey I, Erfle H, Matula P, Kaderali L, Poenisch M, Blankenburg H, Hiet MS, Longerich T, Diehl S, Ramirez F, Balla T, Rohr K, Kaul A, Buhler S, Pepperkok R, Lengauer T, Albrecht M, Eils R, Schirmacher P, Lohmann V, Bartenschlager R.** 2011. Recruitment and activation of a lipid kinase by hepatitis C virus NS5A is essential for integrity of the membranous replication compartment. Cell Host Microbe **9:**32-45.
36. **Chang MH, Gordon LA, Fung HB.** 2012. Boceprevir: a protease inhibitor for the treatment of hepatitis C. Clin Ther **34:**2021-2038.
37. **Wu F, Yang X.** 2003-03-03 2003. A process for preparing 2-trifluoromethyl-10-oxanone from p-trifluorotoluene and o-mercaptobenzoic acid includes nucleophilic substitution reaction on aryl ring to obtain diaryl thioether, and cyclization reaction with concentrated sulfuric acid. China patent 03115623.
38. **Moon JK, Park JW, Lee WS, Kang YJ, Chung HA, Shin MS, Yoon YJ, Park KH.** 1999. Synthesis of some 2-substituted-thioxanthones. J Heterocyclic Chem **36:**793-798.

AAC Accepts published online ahead of print

498 39. **Müller B, Anders M, Akiyama H, Welsch S, Glass B, Nikovics K, Clavel F, Tervo HM,**
499 **Keppler OT, Kräusslich HG.** 2009. HIV-1 Gag processing intermediates trans-dominantly
500 interfere with HIV-1 infectivity. J Biol Chem **284:**29692-29703.
501 40. **Spannaus R, Bodem J.** 2014. Determination of the protease cleavage site repertoire--the
502 RNase H but not the RT domain is essential for foamy viral protease activity. Virology **454-**
503 **455:**145-156.
504
505
506
507
508

AAC Accepts published online ahead of print

509 **FIGURES**

510 **Figure 1. Allosteric site of DENV-3 PR with the docked compounds 3, 6 and 8.** The NS2B unit is
511 shown in green, and the NS3 unit in cyan. Ligands are rendered as CPK-colored sticks with the
512 exception of carbon atoms (**3**: white, **6**: yellow, **8**: pink). Catalytic triad residues His51, Asp75, and
513 Ser135 in the active site, which is behind the allosteric site, are represented in balls and sticks.

514 **Figure 2. Predicted binding modes of compounds 3 and 8**. The PIs were docked into DENV-3 PR
515 by LeadIT-FlexX program. The image was generated with pymol. **(A)** Surface view of the allosteric
516 site with the docked compounds **3** and **8**. Ligands are rendered as CPK-colored sticks with the
517 exception of carbon atoms (**3**: cyan, **8**: pink). **(B)** Binding mode of compound **8** showing the H-bonds
518 between two the hydroxyl groups and the amino acids Lys73, Lys74 and Asn152.

519 **Figure 3. Docking results for PI 6 within the DENV-3 PR. (A)** Three-dimensional interaction
520 diagram of the compound **6** with the amino acids Lys73, Thr120, Asn152 and Gln167. **(B)** Schematic
521 view of all interactions (H-bonds and hydrophobic interactions) of compound **6**.

522 **Figure 4. Inhibition DENV-1 and DENV-2 replication. (A)** Vero cells were pre-incubated with
523 decreasing amounts of the compounds. DMSO served as control. The cells were subsequently infected
524 with DENV-2. Cell culture supernatants were collected and viruses titrated on Vero cells. All
525 experiments were performed in triplicate assays. Error bars represent the standard deviation.
526 Significances of differences in viral titers compared to DMSO control were determined by the paired
527 two-sample t-test and indicated by two asterisks (p-value < 0.01) above the bars. (B) Subtype
528 specificity inhibition of replication by the PIs. Vero cells were pre-incubated with the compounds and
529 infected with DENV-1 or DENV-2 (one genome copy per cell). Cell culture supernatants were
530 collected and viral genome amounts were determined by qRTPCR. All experiments were performed in
531 independent triplicate assays. Error bars represent the standard deviation.

532 **Figure 5. Compounds 3-7 do not influence HIV-1.** HEK 293T cells were transfected with the
533 proviral HIV-1 plasmid pNL4-3 and subsequently incubated with the PIs. Viral titers were determined
534 on TZM-bl indicator cells, which encode a LacZ gene controlled by the HIV-1 LTR promoter. All
535 experiments were performed in triplicate assays. Error bars represent the standard deviation.

AAC Accepts published online ahead of print

536 **Figure 6. Components 1 and 3-7 do not influence HCV replication. (A)** Scheme of the
537 experimental approach. Huh7.5-Fluc cells were transfected with *in vitro* transcribed HCV RNA of the
538 *Renilla* luciferase-encoding reporter virus JcR2a. **(B)** After 72 h virus replication and cell viability
539 were determined by measuring *Renilla* luciferase (Rluc) and Firefly luciferase (Fluc) activity from cell
540 lysates, respectively. **(C)** Production of infectious particles was determined by infection of naïve
541 Huh7.5 cells with supernatants collected from transfected cells and quantification of Rluc activity after
542 72 h. Experiments were performed three times in triplicate (or sextuplicate in the case of DMSO
543 treated cells). The HCV protease inhibitor Boceprevir was included as a positive control. Red line:
544 limit of detection. All data represent the mean of three independent experiments, which were
545 performed in triplicate assays. Error bars represent the standard deviation.

546 **Figure 7. Compounds 1 and 3-7 inhibit DENV-2 PR in cells. (A)** Scheme of the cleavage reporter
547 construct. **(B)** Representative quantitative Western blotting analyses of reporter cleavage by the
548 DENV-2 PR using a monoclonal anti-GFP antibody. Cells were transfected with the reporter vector
549 alone (lane 1), with the PR expression vector alone, or with the reporter vector and the PR (lanes 3 to
550 11). PIs were added after transfection at four non-toxic concentrations (indicated above the panel).
551 Substrate and products were visualized and the inhibition was calculated (ration of (fusion
552 protein)/((fusion protein)+(products)). Expression of the DENV PR was monitored by Western
553 blotting with monoclonal M2-antibodies. The positions of the molecular size markers are indicated.

554

555 **Figure 8. Correlation of antiviral activity** (expressed as log EC_{50}, column 4 in Table 1) **and PR**
556 **inhibition in cell culture** (expressed as log IC_{50}^{incell}, column 5 in Table 1). For the diagram results for
557 compounds **1**, **3**, **4**, **5**, **6**, and **7** were taken.

558

559

AAC Accepts published online ahead of print

560 **TABLES**

561 **Table 1.** Structures and activities of the NS2B/NS3 protease inhibitors

Compound no.	Structure	1 IC_{50},[a] μM DENV-2[e]	2 IC_{50},[a] μM DENV-3[e]	3 Toxicity,[b] [μM]	4 EC_{50},[c] [μM][e]	5 IC_{50},[d] [μM]
1	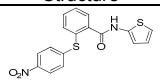	98±4	31.8±4.5	30	3.5±0.3	15.6±3.4
2	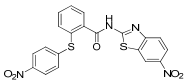	34±5	5.4±2.9	<1	n.d.	n. d.
3	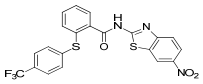	22±1	21±4	1	0.1±0.0	0.2±0.0
4	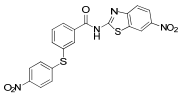	26±1	n.d.	3	0.3±0.1	0.7±0.1
5	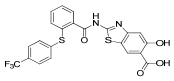	66±3	12.3± 2.2	10	0.9±0.1	2.3±0.7
6	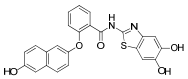	4.2±0.44	0.99±0.1	10	0.8±0.2	3.2±1.2
7	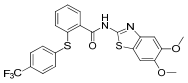	10% inhibition at 50 μM	n.i.	30	2.5±0.1	9.3±2.5
8	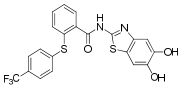	3.6±0.11	9.1±1.02	3	>3	>3

577 [a], inhibition of isolated proteases determined by fluorometric enzymes assays with an AMC derived substrate; [b],
578 concentration, where no influence on cellular metabolism was observed; [c], antiviral activity, inhibition of viral
579 replication; [d], biochemical inhibition of PR in cell culture; n.d., not done; n.i., no inhibition at 50 μM, [e] values are
580 indicated as mean of 3 independent experiments in triplicates ± standard deviation.

AAC Accepts published online ahead of print

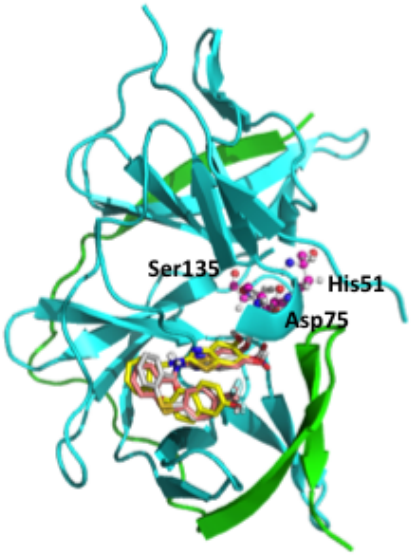

Figure 1. Allosteric site of DENV-3 PR with the docked compounds 3, 6 and 8. The NS2B unit is shown in green, and the NS3 unit in cyan. Ligands are rendered as CPK-colored sticks with the exception of carbon atoms (**3**: white, **6**: yellow, **8**: pink). Catalytic triad residues His51, Asp75, and Ser135 in the active site, which is behind the allosteric site, are represented in balls and sticks.

AAC Accepts published online ahead of print

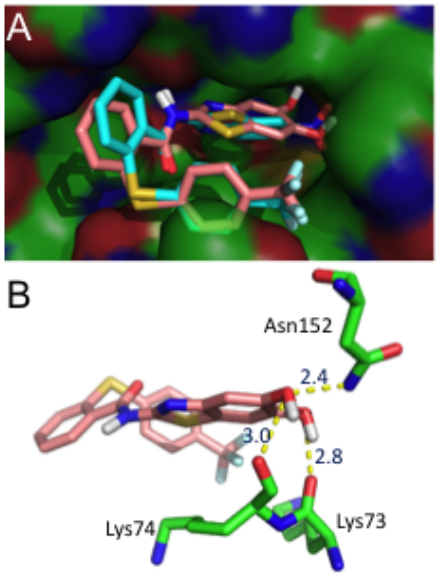

Figure 2. Predicted binding modes of compounds 3 and 8. The PIs were docked into DENV-3 PR by LeadIT-FlexX program. The image was generated with pymol. **(A)** Surface view of the allosteric site with the docked compounds **3** and **8**. Ligands are rendered as CPK-colored sticks with the exception of carbon atoms (**3**: cyan, **8**: pink). **(B)** Binding mode of compound **8** showing the H-bonds between two the hydroxyl groups and the amino acids Lys73, Lys74 and Asn152.

AAC Accepts published online ahead of print

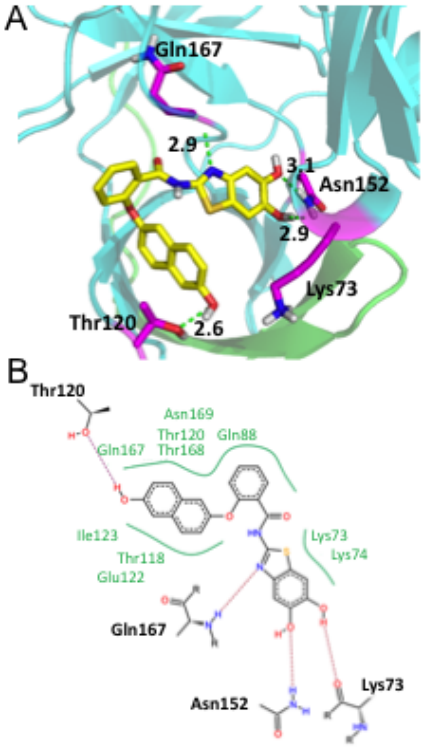

Figure 3. Docking results for PI 6 within the DENV-3 PR. (A) Three-dimensional interaction diagram of the compound **6** with the amino acids Lys73, Thr120, Asn152 and Gln167. **(B)** Schematic view of all interactions (H-bonds and hydrophobic interactions) of compound **6**.

AAC Accepts published online ahead of print

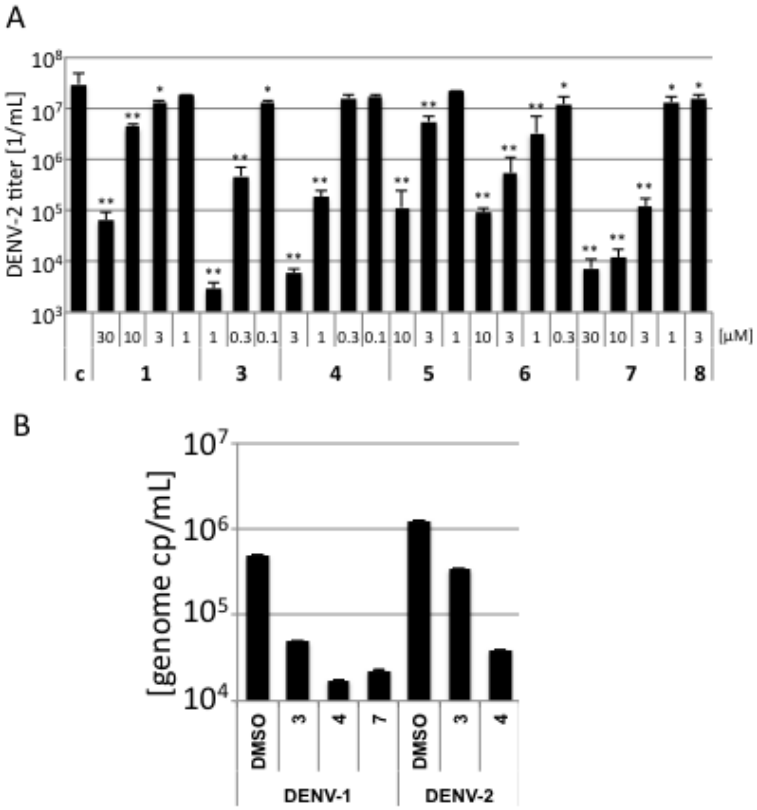

Figure 4. Inhibition DENV-1 and DENV-2 replication. (A) Vero cells were pre-incubated with decreasing amounts of the compounds. DMSO served as control. The cells were subsequently infected with DENV-2. Cell culture supernatants were collected and viruses titrated on Vero cells. All experiments were performed in triplicate assays. Error bars represent the standard deviation. Significances of differences in viral titers compared to DMSO control were determined by the paired two-sample t-test and indicated by two asterisks (p-value < 0.01) above the bars. (B) Subtype specificity inhibition of replication by the PIs. Vero cells were pre-incubated with the compounds and infected with DENV-1 or DENV-2 (one genome copy per cell). Cell culture supernatants were collected and viral genome amounts were determined by qRTPCR. All experiments were performed in independent triplicate assays. Error bars represent the standard deviation.

AAC Accepts published online ahead of print

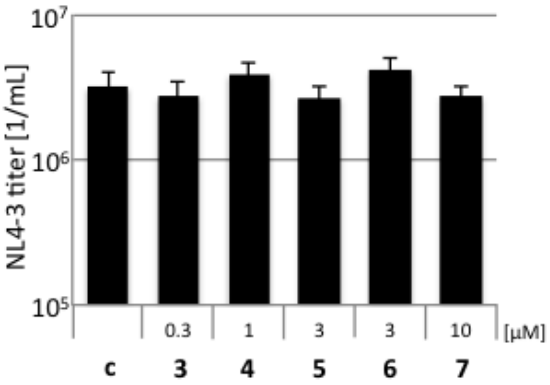

Figure 5. Compounds 3-7 do not influence HIV-1 replication. HEK 293T cells were transfected with the proviral HIV-1 plasmid pNL4-3 and subsequently incubated with the PIs. Viral titers were determined on TZM-bl indicator cells. All experiments were performed in triplicate assays. Error bars represent the standard deviation.

AAC Accepts published online ahead of print

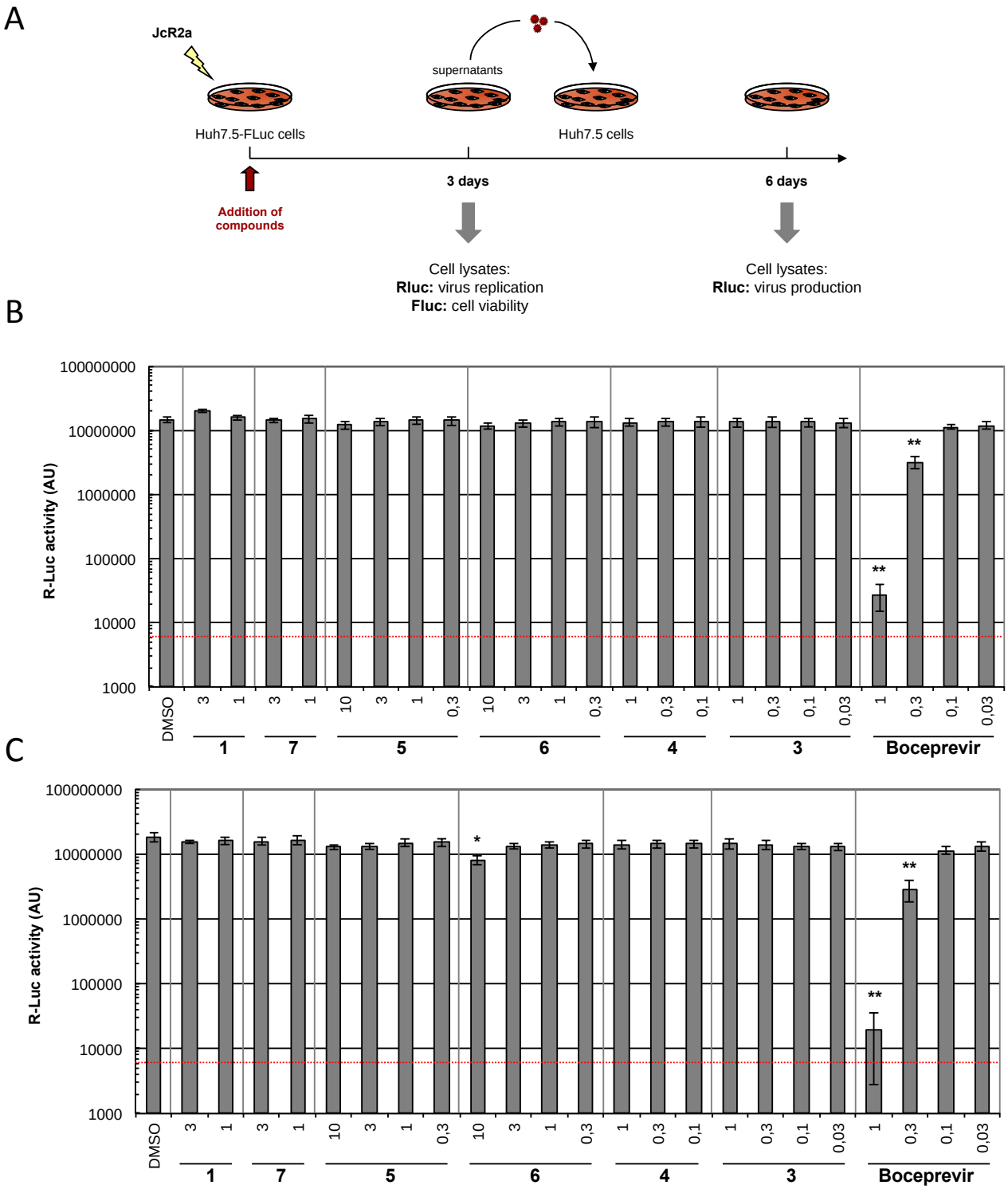

Figure 6. Components 1 and 3-7 do not influence HCV replication. (A) Scheme of the experimental approach. Huh7.5-Fluc cells were transfected with *in vitro* transcribed HCV RNA of the *Renilla* luciferase-encoding reporter virus JcR2a. **(B)** After 72 h virus replication and cell viability were determined by measuring *Renilla* luciferase (Rluc) and Firefly luciferase (Fluc) activity from cell lysates, respectively. **(C)** Production of infectious particles was determined by infection of naïve Huh7.5 cells with supernatants collected from transfected cells and quantification of Rluc activity after 72 h. Experiments were performed three times in triplicate (or sextuplicate in the case of DMSO treated cells). The HCV protease inhibitor Boceprevir was included as a positive control. Red line: limit of detection. All data represent the mean of three independent experiments, which were performed in triplicate assays. Error bars represent the standard deviation.

AAC Accepts published online ahead of print

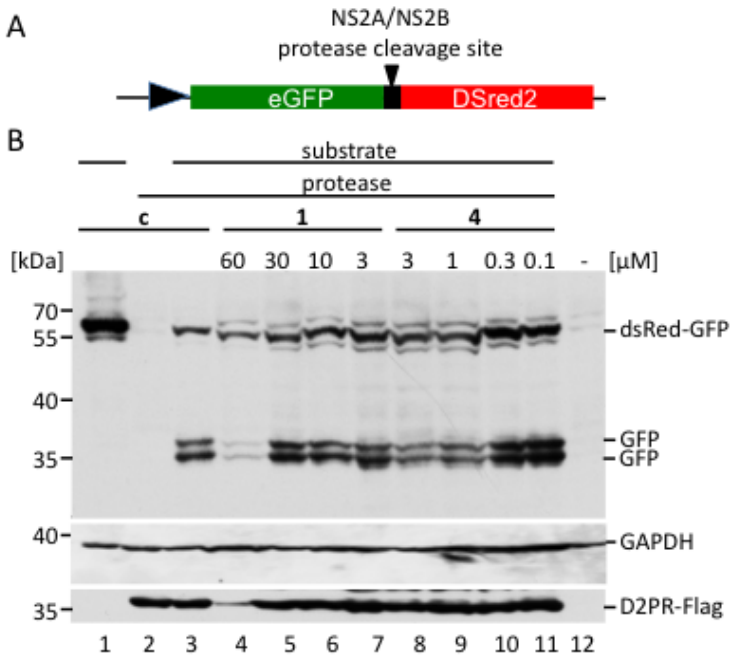

Figure 7. Compounds 1 and 3-7 inhibit DENV-2 PR in cells. (A) Scheme of the cleavage reporter construct. **(B)** Representative quantitative Western blotting analyses of reporter cleavage by the DENV-2 PR using a monoclonal anti-GFP antibody. Cells were transfected with the reporter vector alone (lane 1), with the PR expression vector alone, or with the reporter vector and the PR (lanes 3 to 11). PIs were added after transfection at four non-toxic concentrations (indicated above the panel). Substrate and products were visualized and the inhibition was calculated (ration of (fusion protein)/((fusion protein)+(products)). Expression of the DENV PR was monitored by Western blotting with monoclonal M2-antibodies. The positions of the molecular size markers are indicated.

AAC Accepts published online ahead of print

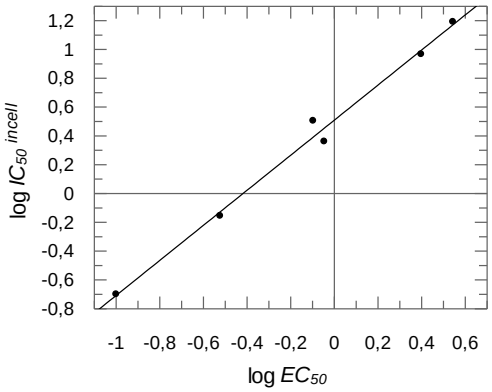

Figure 8. Correlation of antiviral activity (expressed as log EC_{50}, column 4 in Table 1) **and PR inhibition in cell culture** (expressed as log IC_{50}^{incell}, column 5 in Table 1). For the diagram results for compounds **1**, **3**, **4**, **5**, **6**, and **7** were taken.